Intraocular lesions in patients with systemic disease: findings on MR imaging.

H Tonami, H Tamamura, K Kimizu, A Takarada, T Okimura, I Yamamoto and K Sasaki

AJNR Am J Neuroradiol 1989, 10 (6) 1185-1189
http://www.ajnr.org/content/10/6/1185

Intraocular Lesions in Patients with Systemic Disease: Findings on MR Imaging

Hisao Tonami[1]
Hiroyasu Tamamura[1]
Kiyoshi Kimizu[1]
Akira Takarada[1]
Tetsuro Okimura[1]
Itaru Yamamoto[1]
Kazuyuki Sasaki[2]

Twenty-one intraocular lesions associated with various systemic diseases in 15 patients were studied by MR imaging. The disorders included diabetes mellitus, cardiovascular disease, Behçet disease, sarcoidosis, and ankylosing spondylitis. MR was performed on a 0.5-T system using a surface-coil technique. Ophthalmoscopic visualization of the fundus was precluded by the presence of opaque media in all cases.

MR was found to be effective in demonstrating intraocular bleeding, vitreous opacity, detached lesions of the posterior pole, and eyeball deformity. Surface-coil MR is a useful adjunct in the evaluation of the eyes affected by systemic diseases, especially in patients with opaque media.

***AJNR* 10:1185–1189, November/December 1989; *AJR* 154: February 1990**

A wide spectrum of systemic diseases may affect the eyes in a variety of ways [1–3]. Most intraocular conditions can be diagnosed and evaluated by ophthalmoscopic examination. When the ocular media are opaque, however, definitive clinical evaluation of the posterior pole is difficult. In these cases, sonography and CT have been employed, but each has its limitations [4–6].

Recent work with MR imaging using surface coils has suggested that this imaging method has great potential in evaluating diseases of the eye [7–12].

The purpose of this study was to determine the effectiveness of surface-coil MR imaging in the evaluation of eyes affected by various systemic diseases and to clarify the current role of this technique and its limitations.

Subjects and Methods

Surface-coil MR imaging was performed on 15 patients in whom intraocular abnormalities were suspected on the basis of a combination of clinical, ophthalmoscopic, sonographic, and CT findings. The patients were 37 to 78 years old and included six men and nine women. The systemic disorders studied here were diabetes mellitus (eight cases), cardiovascular disease (three), Behçet disease (two), sarcoidosis (one), and ankylosing spondylitis (one). Visualization of the fundus was limited in all 15 patients (17 eyes) by the presence of cataract (three eyes), hyphema (two), vitreous opacity (four), vitreous hemorrhage (five), postsurgical deformity (one), and phthisis bulbi (two).

CT was performed on nine patients with a third-generation scanner.* A 2-mm collimator was used and sections were obtained at 2-mm intervals in axial planes.

MR was performed with a superconducting Siemens unit operating at 0.5 T. The head coil was used for transmission only and a 10-cm-diameter surface coil was placed over the orbits to act as a receiver. The surface coil was positioned parallel to the coronal plane of the orbits to avoid asymmetric signal drop-off or field saturation. T1-weighted spin-echo (SE) images were obtained with 400–600/30–45/2–4 (TR range/TE range/excitations); proton-density- and T2-weighted SE images were obtained with 1600–2000/30–45, 60–90/2.

The majority of studies were begun with axial sections, usually followed by coronal or oblique sagittal sections parallel to the axis of the optic nerve. The section thickness was 5 mm, with a 0–2.5-mm intersection gap. The field of view was 17 cm, and the acquisition

Received October 14, 1988; revision requested December 19, 1988; revision received May 2, 1989; accepted May 10, 1989.

Presented at the annual meeting of the Society of Magnetic Resonance in Medicine, San Francisco, August 1988.

[1] Department of Radiology, Kanazawa Medical University, Uchinada, Kahoku, Ishikawa, 920-02 Japan. Address reprint requests to H. Tonami.

[2] Department of Ophthalmology, Kanazawa Medical University, Ishikawa, 920-02 Japan.

0195-6108/89/1006–1185

* Somatom 2 or Somatom DR 3; Siemens Medical Systems, Iselin, NJ.

matrix was 256 × 256; corresponding pixel size was 0.7 × 0.7 mm. All patients were asked to keep their eyes closed during the examination and to refrain from eye movement.

The MR, CT, sonographic, and ophthalmoscopic examinations were performed within a period of 4 days. Surgery was performed from 2 days to 2 weeks after MR examination, and surgical correlation was available for 13 patients.

TABLE 1: The 21 Intraocular Lesions in 17 Eyes

Systemic Diseases/ Intraocular Lesions	No. of Lesions
Diabetes mellitus	
Vitreous hemorrhage	7
Vitreous opacity	1
Posterior hyaloid detachment	2
Posterior hyaloid hemorrhage	1
Retinal detachment	1
Postsurgical deformity	1
Cardiovascular disease	
Vitreous hemorrhage	1
Vitreous opacity	1
Retinal detachment	1
Subretinal hemorrhage	1
Behçet disease	
Phthisis bulbi	2
Sarcoidosis	
Vitreous opacity	1
Ankylosing spondylitis	
Vitreous opacity	1

Results

Seventeen eyes in 15 patients were affected by systemic diseases in a variety of ways. The 21 intraocular lesions in 17 eyes examined by MR are listed in Table 1. The final diagnoses of these intraocular lesions were made on the basis of surgical findings (13 eyes), or a combination of clinical, sonographic, and CT findings (four eyes).

Intraocular bleeding was present in 10 eyes, including eight vitreous hemorrhages (Fig. 1), one subretinal hemorrhage (Fig. 2) and one posterior hyaloid hemorrhage (Fig. 3). The clinically suspected ages of the hemorrhages ranged from 6 days to 5 months. The hemorrhages were hyperintense on both T1- and T2-weighted images in four eyes (two vitreous hemorrhages, one subretinal hemorrhage, one posterior hyaloid hemorrhage), and the ages of these hemorrhages were from 6 days to 5 months. In two eyes, the vitreous hemorrhages were hyperintense only on T2-weighted images. The ages of the hemorrhages in these cases were 2 months. MR failed to delineate the vitreous hemorrhages in four eyes, and the ages of these hemorrhages were from 3 weeks to 4 months. The documentation of these four vitreous hemor-

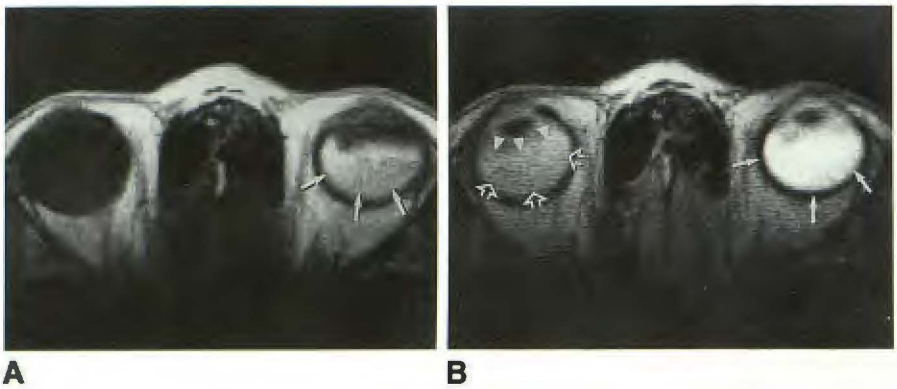

Fig. 1.—Vitreous hemorrhages caused by diabetes mellitus (about 1 week old in the left globe and 2 months old in the right globe).

***A*, Axial T1-weighted image (600/35) shows that vitreous hemorrhage in left globe is hyperintense (*arrows*), while hemorrhage in right globe is hardly recognizable on this image.**

***B*, Hemorrhages are both hyperintense on this axial T2-weighted image (1600/70). Hemorrhage in left globe (*closed arrows*) has a greater intensity than that in right globe (*open arrows*). The presence of hemorrhage in right globe is apparent by the signal difference between vitreous and aqueous humor (*arrowheads*).**

Fig. 2.—Subretinal hemorrhage caused by cardiovascular disease (about 1 month old).

***A*, Noncontrast CT scan shows a diffuse increased density in left globe.**

***B*, Axial T1-weighted image (600/35) demonstrates a hyperintense subretinal hemorrhage. Detached retina is seen as a funnel-shaped configuration (*arrows*).**

C, Subretinal hemorrhage is less conspicuous on this axial T2-weighted image (1600/70). Differentiation from an exudative retinal detachment may be difficult in this subacute stage of hemorrhage.

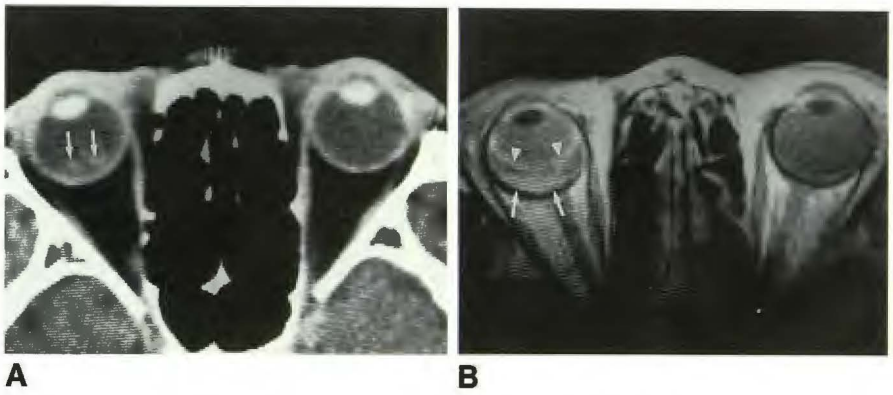

Fig. 3.—Posterior hyaloid hemorrhage caused by diabetes mellitus (about 5 months old).

***A*, Noncontrast CT scan shows slight hyperdensity near posterior pole of right globe (*arrows*).**

***B*, Axial proton-density-weighted image (1600/35) demonstrates a position-dependent hyperintense posterior hyaloid hemorrhage (*arrows*). Thick membrane does not extend to optic disk, indicating posterior hyaloid detachment rather than retinal detachment (*arrowheads*).**

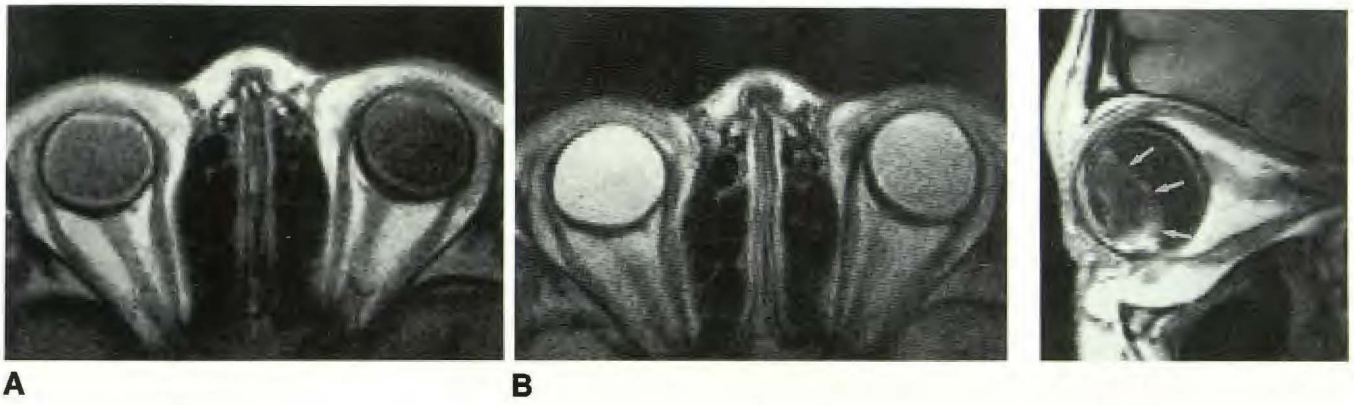

Fig. 4.—Vitreous opacity. The cause of opacity is bleeding into the vitreous by diabetes mellitus.

***A* and *B*, Diseased vitreous in right globe is slightly hyperintense compared with normal in left globe on axial T1-weighted image (600/35) (*A*), but becomes extremely hyperintense on T2-weighted image (1600/70) (*B*). The possibility of magnetic field inhomogeneity can be excluded by a cautious positioning of the surface coil.**

Fig. 5.—Posterior hyaloid detachment caused by diabetes mellitus. Oblique sagittal T1-weighted image (600/40) shows posterior hyaloid detachment as a hyperintense membrane totally detached from posterior pole (*arrows*). Detached membrane does not extend to the optic disk, indicating posterior hyaloid detachment and not retinal detachment.

rhages was made by means of ophthalmoscopy and sonography (three eyes), or sonography only (one eye). Surgical confirmations were obtained in all four patients, and the time between MR and surgery was from 4 days to 2 weeks.

Vitreous opacity was present in four eyes. The causes of opacity were bleeding into the vitreous in two eyes and exudation of inflammatory cells by uveitis in two eyes. Three of four vitreous opacities were hyperintense on T2-weighted images (Fig. 4), but MR failed to demonstrate the lesion in one eye. The cause of this opacity was bleeding into the vitreous caused by cardiovascular disease.

Detached lesions of the posterior pole were present in four eyes, two with retinal detachment and two with posterior hyaloid detachment. All four lesions were clearly demonstrated on MR. Oblique sagittal sections parallel to the axis of the optic nerve were most useful for differentiating between these two lesions. MR depicted subretinal effusion or hemorrhage as a funnel-shaped hyperintensity with its apex at the optic disk and its extremities pointed toward the ciliary body (see Fig. 6C), while posterior hyaloid detachment was demonstrated as a thick membrane that was totally detached from the posterior pole (Fig. 5).

Deformity and decreased size of the globe were present in three eyes, two phthisis bulbi and one postsurgical deformity. MR clearly demonstrated the complicated inner structures (Figs. 6 and 7).

Discussion

The majority of intraocular lesions associated with systemic diseases can be diagnosed accurately by ophthalmoscopic examination, unless the ocular media are opaque. Most of the systemic diseases, however, have a tendency to affect the ocular media, such as the cornea, lens, and vitreous [1]. Thus, direct visualization of the fundus is sometimes hampered and misdiagnosis is possible. On these occasions, sonography and CT have been the main alternative imaging methods.

Ocular sonography is now a well-established technique, but its use is limited in certain situations, such as diffuse vitreous

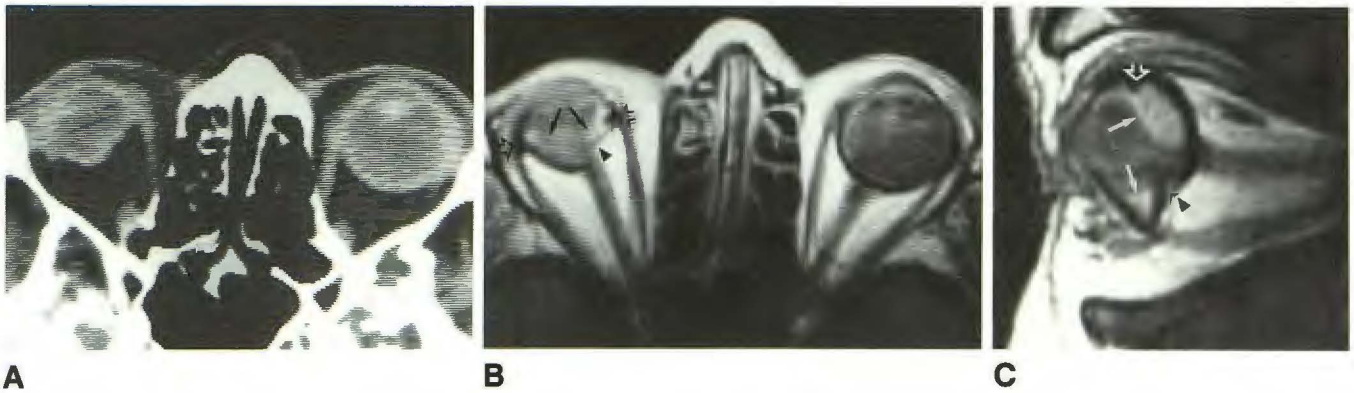

Fig. 6.—Postsurgical deformity. This patient had lensectomy, vitrectomy, and scleral banding in the right globe.
***A*, Noncontrast CT scan shows decreased size and deformity of right globe.**
***B* and *C*, Axial T1-weighted image (600/35) (*B*) and oblique sagittal T1-weighted image (600/40) (*C*) clearly show retinal detachment (*closed arrows*) and disruption of sclera (*arrowheads*). Retinal detachment is demonstrated as a funnel-shaped configuration with its apex at the optic disk. Silicone rubber implants are seen as a hypointensity (*open arrows*).**

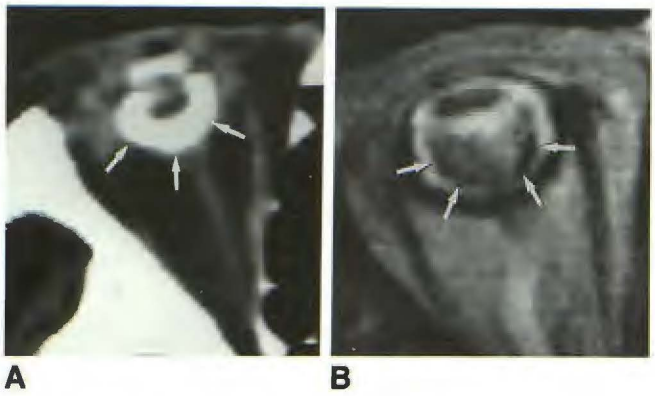

Fig. 7.—Phthisis bulbi.
***A*, Noncontrast CT scan shows right globe to be small and deformed with peripheral calcification (*arrows*).**
***B*, Axial T2-weighted image (1600/70) shows subretinal calcification as a V-shaped hypointensity (*arrows*).**

hemorrhage or vitritis, and dense intraocular calcification [4, 5]. Furthermore, it is relatively operator-dependent and is not tolerated by a patient with a painful eye.

CT also has several limitations. It is relatively nonspecific in respect to tissue characterization, and it sometimes fails to demonstrate certain intraocular conditions themselves [13–17]. Among nine patients who had CT examinations in our study, only three were diagnosed correctly on CT. In two of the remaining six, CT misdiagnosed subretinal hemorrhage (Fig. 2A) and posterior hyaloid hemorrhage (Fig. 3A) as vitreous hemorrhage, and failed to demonstrate the lesions themselves in four patients (two with vitreous hemorrhage and two with vitreous opacity). Furthermore, the radiation dose associated with high-resolution CT studies is significant, and repeated examinations can approach a level known to induce cataract [18].

MR with the use of surface coils is extremely attractive for the evaluation of intraocular conditions because of its noninvasiveness, absence of ionizing radiation, multiplanar capability, and excellent tissue contrast. Even in our limited series of 15 patients, MR has demonstrated its ability to delineate intraocular conditions and has proved to be useful for the evaluation of eyes affected by systemic diseases. As the patient population increases, more information will be available, but some valuable clinical correlations and characteristic MR findings have been noted.

Hemorrhagic collections have a varied appearance on MR, depending on the state of hemoglobin [19]. In our series, however, no apparent correlation between the MR signal changes and the ages of the hemorrhages could be found. It seems that this inconsistency is derived from the uncertainty of the ages of the hemorrhages, since the time elapsed after hemorrhage was estimated from the onset of the clinical symptoms in most cases. Furthermore, the hemorrhages associated with systemic diseases tend to be repetitive and this also makes it difficult to establish their age.

In three of four eyes with vitreous opacity, the diseased vitreous appeared hyperintense relative to normal on T2-weighted images. This is believed to be the result of released protein-laden exudate into the vitreous [15, 20–22]. This kind of unilateral hyperintensity may be the result of magnetic-field inhomogeneity. In our series, however, the possibility of magnetic-field inhomogeneity could be excluded, since the surface coil was positioned cautiously to avoid asymmetric signal drop-off or field saturation.

Retinal detachment and posterior hyaloid detachment can be differentiated from each other on MR. Retinal detachment is depicted as a funnel-shaped configuration with its apex at the optic disk and its extremities pointed toward the ciliary body [23]. Although the retina itself is very thin, measuring 0.5 mm near the disk to 0.1 mm anteriorly, and is beyond the limit of resolution of MR, it is seen when outlined by the significant contrast difference between the hyperintense subretinal effusion or hemorrhage and the hypointense vitreous cavity [23, 24].

On the other hand, posterior hyaloid detachment is seen as a thick hyperintense membrane totally detached from the posterior pole, unlike the retinal detachment. Although the posterior hyaloid membrane is also very thin and invisible on

MR, it can be made visible when blood fills the posterior hyaloid space, causing thickening of this membrane [23]. Oblique sagittal sections parallel to the axis of the optic nerve are particularly useful for differentiating between the two lesions, because these sections provide realistic information about the relationship between the detached lesion and the optic disk.

MR is also useful for evaluating deformity and dimensional changes of the eye [15]. It is well suited for demonstration of organized retinal detachment, cicatrization, and focal deformation. Although MR has a limited ability to identify calcification, the thick subretinal calcification was depicted as a V-shaped hypointensity in a case of phthisis bulbi (Fig. 7B).

In summary, surface-coil MR can produce high-quality images of a variety of intraocular lesions. In the presence of opaque media, this technique provides valuable information about the condition of the posterior pole not available on the ophthalmoscopic examination. The results of our study suggest that surface-coil MR may become a useful adjunct in the evaluation of eyes affected by systemic diseases.

Further study will be needed to assess the precise correlation between the evolution of intraocular bleeding and the MR signal characteristics.

ACKNOWLEDGMENTS

We thank Akiko Ohta for secretarial help, Tomokazu Oku and Masao Yonezawa for technological assistance, and James C. Ehrhardt for manuscript review.

REFERENCES

1. Mansolf FA. *The eye and systemic disease*. St. Louis: Mosby, **1980**
2. Gittinger JW. *Ophthalmology: a clinical introduction*. Boston: Little, Brown, **1984**
3. Newell FW. *Ophthalmology: principles and concepts*. St. Louis: Mosby, **1986**
4. Innes J, McCreath G, Forrester JV. Ultrasonic pattern in vitreo-retinal disease. *Clin Radiol* **1982**;33:585–591
5. Zakov ZN, Berlin LA, Gutman FA. Ultrasonographic mapping of vitreoretinal abnomalities. *Am J Ophthalmol* **1983**;96:622–631
6. Osborne DR, Foulks GN. Computed tomographic analysis of deformity and dimensional changes in the eyeball. *Radiology* **1984**;153:669–674
7. Zimmerman RA, Bilaniuk LT, Yanoff M, et al. Orbital magnetic resonance imaging. *Am J Ophthalmol* **1985**;100:312–317
8. Bilaniuk LT, Schenck JF, Zimmerman RA, et al. Ocular and orbital lesions: surface coil MR imaging. *Radiology* **1985**;156:669–674
9. Gomori JM, Grossman RI, Shields JA, et al. Choroidal melanomas: correlation of NMR spectroscopy and MR imaging. *Radiology* **1986**;158:443–445
10. Gomori JM, Grossman RI, Shields JA, et al. Ocular MR imaging and spectroscopy: an ex vivo study. *Radiology* **1986**;160:201–205
11. Atlas SW, Bilaniuk LT, Zimmerman RA, et al. Surface coil spin-echo MR imaging of the orbit at 1.5T: initial experience. *Radiology* **1987**;164:501–509
12. Tonami H, Nakagawa T, Yamamoto I, et al. MR imaging of a morning glory syndrome. *J Comput Assist Tomgr* **1987**;11:529–530
13. Mafee MF, Peyman GA, McKusick MA. Malignant uveal melanoma and similar lesions studied by computed tomography. *Radiology* **1985**;156:403–408
14. Peyster RG, Angsburger JJ, Shields JA, et al. Choroidal melanoma: comparison of CT, fundoscopy, and US. *Radiology* **1985**;156:675–680
15. Haik BG, St. Louis L, Smith ME, et al. Magnetic resonance imaging in the evaluation of leukocoria. *Ophthalmology* **1985**;92:1143–1152
16. Worthington BS, Wright JE, Curati WL, et al. The role of magnetic resonance imaging techniques in the evaluation of orbital and ocular disease. *Clin Radiol* **1986**;37:219–226
17. Mafee, MF, Peyman GA, Grisolano JE, et al. Malignant uveal melanomas and simulating lesions: MR imaging evaluation. *Radiology* **1986**;160:773–780
18. Lund E, Halaburt M. Irradiation dose to the lens of the eye during CT of the head. *Neuroradiology* **1982**;22:181–184
19. Gomori JM, Grossman RI, Goldberg HI, et al. Intracranial hematomas: imaging by high-field MR. *Radiology* **1985**;157:87–93
20. Gonzalez RG, Cheng H-M, Barnett P, et al. Nuclear magnetic resonance imaging of the vitreous body. *Science* **1984**;223:399–400
21. terPenning BJ, Cheng H-M, Barnett P, et al. MR imaging of enucleated human eyes at 1.4 tesla. *J Comput Assist Tomogr* **1986**;10:551–559
22. Aquayo J, Glaser B, Mildvan A, et al. Study of vitreous liquifaction by NMR spectroscopy and imaging. *Invest Ophthalmol Vis Sci* **1985**;26:692–697
23. Mafee MF, Peyman GA. Retinal and choroidal detachment: role of magnetic resonance imaging and computed tomography. *Radiol Clin North Am* **1987**;25:387–507
24. Okabe H, Kizosawa M, Yamada S, et al. Nuclear magnetic resonance imaging of subretinal fluid. *Am J Ophthalmol* **1986**;102:640–646